small structures
www.small-structures.com

$Sr(NO_3)(NH_2SO_3)\cdot H_2O$: First Nitrate Sulfamate Revealing Remarkable Second Harmonic Generation and Optimized Birefringence

Xuefei Wang, Yang Li, Zilong Chen, Jihyun Lee, Fangfang Zhang, Kenneth R. Poeppelmeier, Shilie Pan,* and Kang Min Ok**

The approach of synergistically combining mixed chromophores has garnered significant attention attributed to its ability to leverage the advantages of both groups and design novel nonlinear optical (NLO) materials. Herein, $Sr(NO_3)(NH_2SO_3)\cdot H_2O$, a noncentrosymmetric compound, which represents the first reported nitrate sulfamate compound, is successfully designed and synthesized. The compound features zigzag $[SrNO_{10}(H_2O)]_\infty$ infinite layers, forming a honeycomb-like graphene topology in its layered structure. The unique arrangement results in an excellent second harmonic generation response, 5.1 times that of KH_2PO_4, and an optimized birefringence of 0.06650 at 532 nm. In addition, the presence of interlayered covalent $[NH_2SO_3]$ groups facilitates improved crystal growth habits, resulting in a large single crystal measuring $19.0 \times 17.0 \times 3.5$ mm^3. In this discovery, a new class of NLO materials is introduced and the scope of structural chemistry is significantly expanded.

Nonlinear optical (NLO) crystals have garnered significant interest owing to their wide-ranging applications in optical communications, all-solid-state lasers, and advanced scientific instruments.[1] In recent decades, researchers have discovered numerous materials with excellent NLO properties suitable for ultraviolet (UV) frequency doubling.[2] These materials are primarily found in systems that incorporate π-conjugated units such as borates, nitrates, and carbonates, as well as systems with symmetric tetrahedra such as phosphates and sulfates.[3] It has been demonstrated that materials featuring well-regulated π-conjugated units, such as $[BO_3]$, $[CO_3]$, and $[NO_3]$, arranged in parallel, exhibit significant anisotropy, resulting in a pronounced second harmonic generation (SHG) response and moderate birefringence for phase matching (PM).[4] Conversely, compounds containing $[SO_4]$ and $[PO_4]$ tetrahedra with large highest occupied molecular orbital (HOMO)−least unoccupied molecular orbital (LUMO) gaps typically demonstrate broader UV transparency windows.[5] However, materials with only one type of anionic group often possess inherent limitations, such as layered growth habits for parallel triangular units or relatively small birefringence for tetrahedral units.[6] Therefore, it is reasonable to explore compounds with mixed anionic groups, harnessing the merits of different anionic groups to compensate for their respective weaknesses.

The incorporation of different anionic groups presents a versatile strategy for achieving various objectives in the design of NLO materials.[7] The synergistic effects resulting from the combination of these groups can lead to materials with significantly improved NLO properties. For instance, compounds that feature combinations of two π-conjugated anionic groups, such as $Pb_2(BO_3)(NO_3)$ and $Pb_7O(OH)_3(CO_3)_3(BO_3)$, or combinations of stereoactive and π-conjugated anionic groups, such as $PbCdF(SeO_3)(NO_3)$ and $Sc(IO_3)_2(NO_3)$, have demonstrated enhanced SHG responses and birefringence.[8] Furthermore, the utilization of mixed anionic groups can aid in optimizing overall properties, as evidenced by fluorooxoborates, borophosphates, and borosilicates.[9] Notable examples of this approach include deep-UV NLO materials such as AB_4O_6F ($A = NH_4$, K, Rb, Cs), $(NH_4)_3B_{11}PO_{19}F_3$, $Ba_3(ZnB_5O_{10})PO_4$, and $Cs_2B_4SiO_9$.[10] In recent years, metal sulfamates have emerged as promising NLO candidates due to the highly anisotropic nature of their asymmetric $[NH_2SO_3]$ tetrahedral group.[11]

X. Wang, Y. Li, J. Lee, K. M. Ok
Department of Chemistry
Sogang University
Seoul 04107, Republic of Korea
E-mail: kmok@sogang.ac.kr

Z. Chen, F. Zhang, S. Pan
Research Center for Crystal Materials
CAS Key Laboratory of Functional Materials and Devices for Special Environments
Xinjiang Technical Institute of Physics & Chemistry
CAS
Urumqi 830011, P. R. China
E-mail: slpan@ms.xjb.ac.cn

K. R. Poeppelmeier
Department of Chemistry
Northwestern University
Evanston, IL 60208, USA
E-mail: krp@northwestern.edu

The ORCID identification number(s) for the author(s) of this article can be found under https://doi.org/10.1002/sstr.202300274.

DOI: 10.1002/sstr.202300274

The tetrahedral unit offers remarkable hyperpolarizability while maintaining a large HOMO–LUMO gap, making it an ideal candidate for UV NLO applications. To further enhance their SHG and birefringent abilities, designing new materials with mixed anionic groups based on sulfamates represents a promising approach. Recently, Tian et al. has developed a co-crystal, $KNO_3SO_3NH_3$, by introducing KNO_3 into the centrosymmetric SO_3NH_3 crystal, thus offering the possibility of combining $[NO_3]$ anionic units with $[NH_2SO_3]$ groups.[12]

By drawing upon these chemical motivations, we endeavored to combine the π-conjugated $[NO_3]$ and asymmetric $[NH_2SO_3]$ tetrahedral anionic groups in the design of new NLO materials, resulting in the successful synthesis of the first nitrate sulfamate, $Sr(NO_3)(NH_2SO_3)\cdot H_2O$, with a honeycomb-like topology in its layered structure. The arrangement within the new compound is beneficial for SHG, leading to an exceptional SHG response of 5.1 times that of KH_2PO_4 (KDP), as well as an enhanced yet optimized birefringence of 0.06650 at 532 nm. Additionally, the presence of interlayered covalent $[NH_2SO_3]$ groups promotes improved crystal growth habits, resulting in single crystals with the largest dimensions of $19.0 \times 17.0 \times 3.5$ mm^3 (Figure S1, Supporting Information). This discovery introduces a new class of NLO materials and expands the scope of structural chemistry.

$Sr(NO_3)(NH_2SO_3)\cdot H_2O$ crystallizes in the noncentrosymmetric (NCS) polar space group, $Pca2_1$ with the orthorhombic system. Our objective was to combine the π-conjugated $[NO_3]$ and asymmetric $[NH_2SO_3]$ tetrahedral anionic groups in the design of new NLO materials, leading to the successful growth of the first nitrate sulfamate crystal, $Sr(NO_3)(NH_2SO_3)\cdot H_2O$, with promising UV NLO properties. The unit cell consists of one Sr atom, one S atom, two N atoms, and seven O atoms, each in independent crystallographic positions. The $[SrO_9(H_2O)]$ polyhedra are formed by the coordination of the Sr1 atom with ten O atoms, with Sr−O lengths ranging from 2.502(5) to 2.814(6) Å (Figure S2, Supporting Information). The N1 atoms coordinate with three O atoms to form the triangular $[NO_3]$ units, with N−O distances ranging from 1.234(7) to 1.281(6) Å. The $[NH_2SO_3]$ tetrahedra group is formed by the coordination of the S1 atom with three O atoms and one N2 atom, with S−O and S−N lengths from 1.448(5) to 1.465(5) Å and 1.640(7) Å, respectively. All bond lengths and coordination environments are consistent with reported structures.[13] The layered structure of $Sr(NO_3)(NH_2SO_3)\cdot H_2O$ is illustrated in **Figure 1**a, with interlayer $[NH_2SO_3]$ tetrahedra sandwiched between layers composed of $[SrO_9(H_2O)]$ polyhedra and $[NO_3]$ units. These layers are connected by sharing two edge oxygens, forming a zigzag $[SrNO_{10}(H_2O)]_\infty$ infinite layer with adjacent $[NO_3]$ dihedral angles of 33.3(3)° and 49.2(3)° (Figure S3 and S4, Supporting Information). To gain a better understanding of the layered structure, a topological analysis was conducted. The honeycomb-like topology in the $[SrNO_{10}(H_2O)]_\infty$ layer is a beneficial structural feature that facilitate the regulation of anionic group arrangements into an in-phase configuration, thus enhancing the SHG response and birefringence (Figure 1b). This observation is supported by reported NLO materials with similar structures, such as $LiCs_2PO_4$, $CsNaMgP_2O_7$, and Hg_3AsSe_4X (X = Br, I).[14] The $[NH_2SO_3]$ tetrahedra are arranged with alternating directions to interconnect neighboring layers (Figure S5, Supporting Information). The angle between adjacent $[NH_2SO_3]$ tetrahedra was determined to be 67.7(3)° (Figure S6, Supporting Information). It is worth noting that the covalent $[NH_2SO_3]$ groups play a significant role in tightly connecting the $[SrNO_{10}(H_2O)]_\infty$ layers, resulting in desirable crystal growth habits. This characteristic enables the growth of $Sr(NO_3)(NH_2SO_3)\cdot H_2O$ crystals with a thickness of 3.5 mm along the *b*-axis.

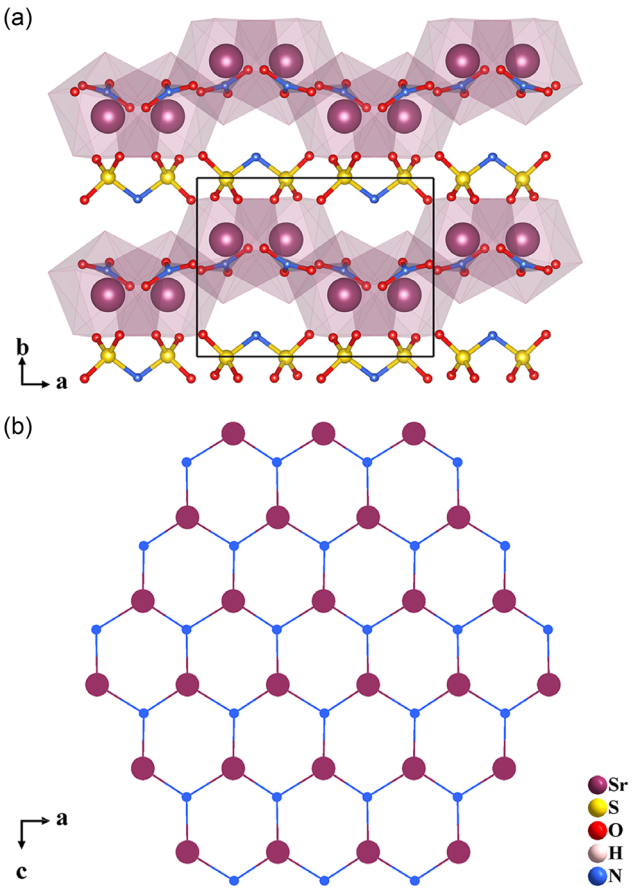

Figure 1. a) Crystal structure of $Sr(NO_3)(NH_2SO_3)\cdot H_2O$ viewed along the *c*-axis. b) Topological graph of $[SrNO_{10}(H_2O)]_\infty$ layer viewed along the *b*-axis.

The experimental powder X-Ray diffraction (PXRD) pattern matches well with the one simulated from single-crystal X-Ray diffraction (SC-XRD) (**Figure 2**a). Further validation of the fit quality was performed by conducting a Rietveld refinement analysis (Figure S7, Supporting Information). The thermogravimetric analysis (TGA) reveals that $Sr(NO_3)(NH_2SO_3)\cdot H_2O$ exhibits thermal stability up to 130 °C (Figure 2b). Upon further heating, a weight loss of 6.6% was observed, corresponding to the release of molecular water and in good agreement with the theoretical weight loss of 6.8%. A second stage of weight loss occurred at 230 °C, with approximately 21.8% of the total weight being lost due to the evaporation of nitrogen-containing gas. A minor weight loss was observed at 546 °C, and the weight stabilized at 69.5%, consistent with the theoretical residual weight of 69.6% based on $SrSO_4$. To investigate the possible anhydrous

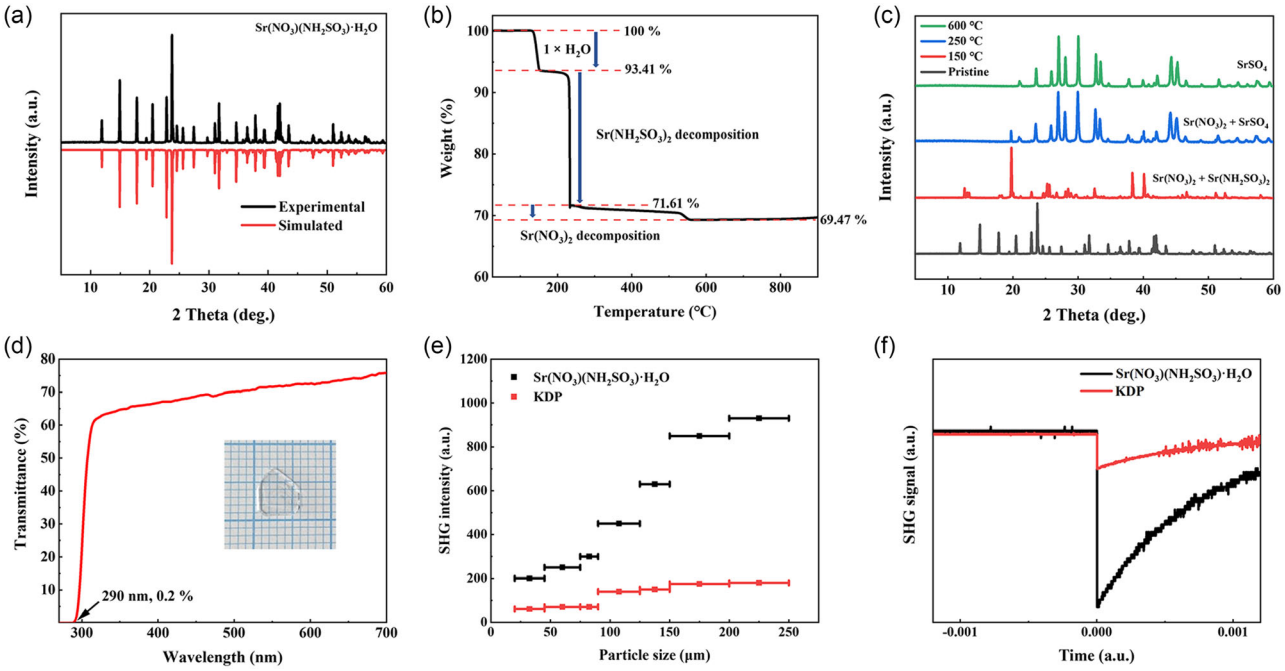

Figure 2. a) Comparison of experimental and simulated powder X-Ray diffraction (PXRD) patterns, b) thermogravimetric analysis (TGA) diagram, c) ex situ PXRD patterns at various temperatures, d) UV–vis transmittance spectrum collected from the single crystal, e) powder second harmonic generation (SHG) measurements at 1064 nm, and f) oscilloscope traces compared with the KH_2PO_4 sample in the range of 200−250 μm for $Sr(NO_3)(NH_2SO_3)\cdot H_2O$.

phase of $Sr(NO_3)(NH_2SO_3)\cdot H_2O$ and confirm its decomposition products, *ex situ* PXRD patterns of samples annealed at various temperatures were collected (Figure 2c). The results revealed that the sample heated at 150 °C for 12 h underwent direct decomposition into $Sr(NO_3)_2$ and $Sr(NH_2SO_3)_2$, while samples heated at 250 °C for 12 h showed the presence of $Sr(NO_3)_2$ and $SrSO_4$. Finally, samples heated at 600 °C for 12 h exhibited characteristic peaks of $SrSO_4$ only. These findings provide insight into the stability of $Sr(NO_3)(NH_2SO_3)\cdot H_2O$ and its decomposition pathway.

The linear optical and NLO properties of $Sr(NO_3)(NH_2SO_3)\cdot H_2O$ were characterized to assess its transparent window and SHG capability. The UV–vis diffuse reflectance spectrum reveals no noticeable absorption between 320 and 800 nm except for a wide absorption band with a peak at 273 nm (Figure S8a, Supporting Information). The UV cutoff edge was determined to be at 231 nm with a reflectance of 18%. The absorbance curve was transformed by the Kubelka–Munk functions.[15] The transformed absorbance curve and the corresponding bandgap of 4.99 eV are presented in Figure S8b (Supporting Information). To evaluate the practical transparency window of $Sr(NO_3)(NH_2SO_3)\cdot H_2O$, the transmission spectrum was obtained by measuring the transmittance of a polished crystal. The transmittance remained above 60% up to 300 nm, and a sharp cutoff edge at 290 nm, indicating a bandgap of 4.10 eV (Figure 2d and S8c, Supporting Information). According to the comparison, the diffuse reflectance spectrum overestimates the actual UV transparent window attributed to the overlooked intrinsic absorption band for $[NO_3]$ groups, which was also observed in another reported nitrate.[16] The infrared spectrum of $Sr(NO_3)(NH_2SO_3)\cdot H_2O$ was collected to identify its anionic groups. The absorption peaks were assigned by comparing them with reported spectra of nitrates and sulfamates (Figure S9 and Table S5, Supporting Information).[4a,13b] The SHG ability of $Sr(NO_3)(NH_2SO_3)\cdot H_2O$ was assessed using the Kurtz–Perry method, comparing it with the benchmark material KDP under a 1064 nm fundamental laser (Figures 2e,f).[17] The results indicate that $Sr(NO_3)(NH_2SO_3)\cdot H_2O$ exhibits type I PM with increasing particle sizes and SHG responses. In the particle size range of 200–250 μm, $Sr(NO_3)(NH_2SO_3)\cdot H_2O$ demonstrates approximately 5.1 times higher SHG response than KDP, highlighting its exceptional frequency-doubling capability.

The crystal used for birefringence measurement was identified as a (010) crystal wafer (Figure S10a, Supporting Information). Optical analysis under a cross-polarized microscope reveals a typical conoscopic interference pattern with two distinct melatopes, indicating that the crystal is biaxial. This observation confirms the determined space group of $Pna2_1$ by SC-XRD (Figure S10b, Supporting Information). The refractive indices of $Sr(NO_3)(NH_2SO_3)\cdot H_2O$ were measured along the three principal axes using the prism coupling method by employing polarized lasers with TE (electric field transverse to the plane of incidence) and TM (magnetic field transverse to, and electric field parallel to the plane of incidence) incidence. Five light sources with varying wavelengths were employed for the measurements. The obtained values were then fitted using the Sellmeier equation (Table S6 and S7, Supporting Information). The fitted chromatic dispersion curves illustrate the relationship of $n_z - n_y < n_y - n_x$, indicating that

$Sr(NO_3)(NH_2SO_3)\cdot H_2O$ is a negative biaxial crystal with a birefringence ($\Delta n = n_z - n_x$) ranging from 0.05709 to 0.07077 over the measured range (**Figure 3**a). For type I SHG PM condition, the equation of $n(\omega) = n(2\omega)$ must be satisfied. The UV PM limit can be determined from the intersection of the $n_z(\omega)$ and $n_x(2\omega)$ curves. Based on the analysis, the shortest type I SHG PM wavelength of $Sr(NO_3)(NH_2SO_3)\cdot H_2O$ is estimated to be 291 nm. In the case of type I third harmonic generation (THG), the PM condition follows the equation, $n_z(\omega) + 2n_z(2\omega) = 3n_x(3\omega)$. The theoretically shortest type I THG PM wavelength for $Sr(NO_3)(NH_2SO_3)\cdot H_2O$ is determined to be 285 nm (Figure 3b). Considering the UV cutoff edge, $Sr(NO_3)(NH_2SO_3)\cdot H_2O$ is expected to be capable of generating coherent light at wavelength above 290 nm through the THG process. Additionally, the PM angles (θ, ϕ) on the three principal planes (*X*–*Y*, *Y*–*Z*, and *X*–*Z*) for SHG and THG were evaluated (Figure 3c,d). The type II PM wavelength limits for SHG and THG were also determined. The calculated values are 354 nm for SHG at $\theta = 0°$, $\phi = 90°$ in the *X*–*Y* plane, and 310 nm for THG at $\theta = 0°$, $\phi = 90°$ in the *X*–*Y* plane. The incorporation of π-conjugated $[NO_3]$ anionic groups into the sulfamate system leads to a significant enhancement of birefringence in $Sr(NO_3)(NH_2SO_3)\cdot H_2O$ compared to other sulfamates. These findings suggest a favorable potential for coherent light output at 355 nm using multiple critical PM approaches for $Sr(NO_3)(NH_2SO_3)\cdot H_2O$.

The synergistic combination of $[NO_3]$ and $[NH_2SO_3]$ groups in $Sr(NO_3)(NH_2SO_3)\cdot H_2O$ results in promising optical performance. A comparison of the optical properties between NCS sulfamates and nitrates is presented in Table S8.[4a,9a,9b,11b,12,16,18] The sulfamates exhibit wide bandgaps, along with relatively small birefringences and SHG responses. In the case of nitrates, the presence of $[NO_3]$ groups results in strong SHG responses and improved birefringences for several compounds. However, the narrow bandgaps and limited UV transparency windows of nitrates constrain their potential applications. The incorporation of $[NO_3]$ groups significantly enhances the SHG response of $Sr(NO_3)(NH_2SO_3)\cdot H_2O$ compared to NCS sulfamates, allowing it to achieve a comparable SHG response to nitrate-based NLO materials (**Figure 4**a). Additionally, the inclusion of $[NH_2SO_3]$ groups expands the UV transparent window of $Sr(NO_3)(NH_2SO_3)\cdot H_2O$. To assess the performance, the absorption edges were considered due to the overestimation of the cutoff edge in diffuse reflectance spectra for nitrates. The average absorption edges of NCS nitrates were found to be 319 nm, while the absorption edge of $Sr(NO_3)(NH_2SO_3)\cdot H_2O$ is extended and blueshifted to 300 nm, making $Sr(NO_3)(NH_2SO_3)\cdot H_2O$ suitable for UV applications. The moderate birefringence is crucial for PM and efficient laser output in NLO materials. According to a previous study by Tran et al., deep-UV NLO materials typically exhibit a moderate birefringence in the range of 0.07–0.10. For the IR and visible regions, a relatively small birefringence

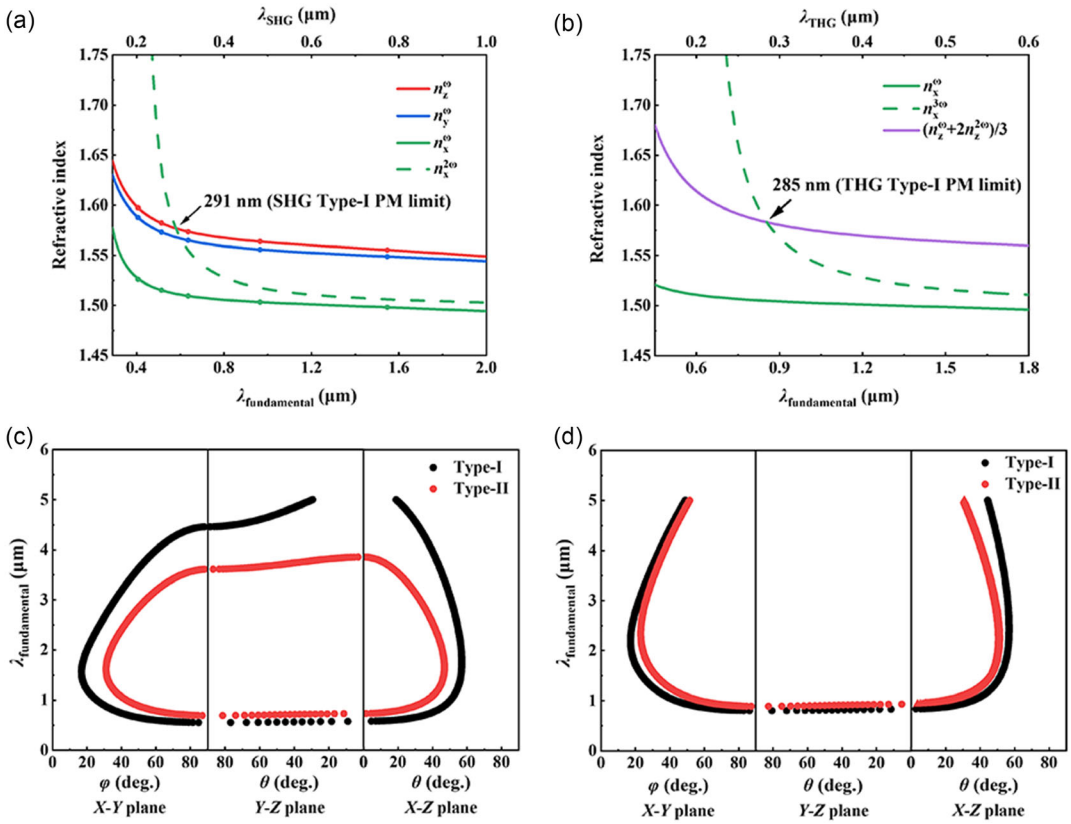

Figure 3. a) The fitted chromatic dispersion curves for fundamental and second-harmonic light, b) third-harmonic light, c) calculated SHG phase matching (PM) angles, and d) calculated third harmonic generation (THG) PM angles ϕ and θ for $Sr(NO_3)(NH_2SO_3)\cdot H_2O$.

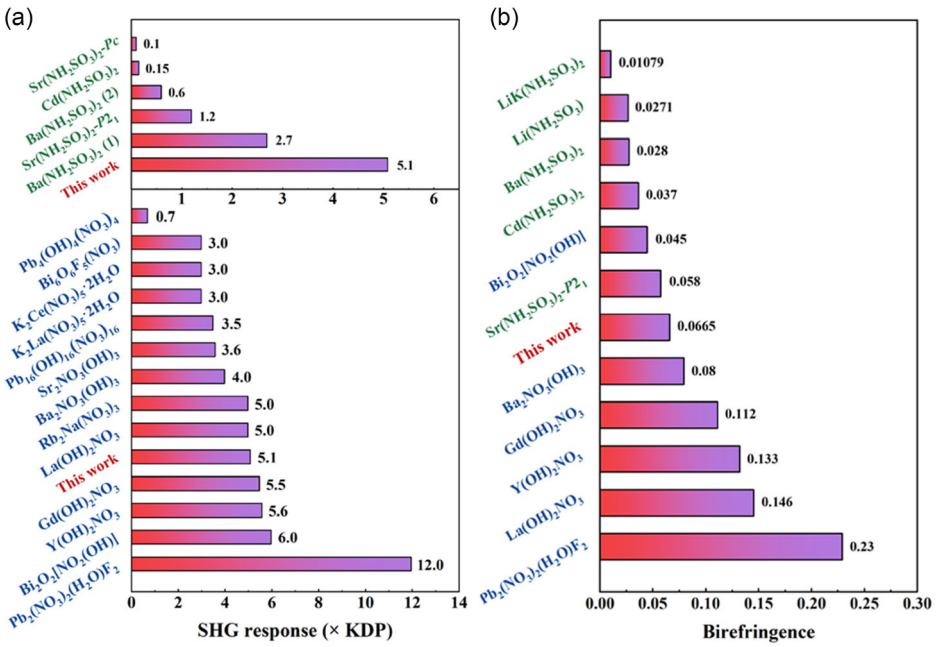

Figure 4. The comparisons of a) SHG responses and b) birefringence of NCS sulfamates, nitrates, and nitrate sulfamates.

of approximately 0.03 is sufficient to achieve the PM condition.[19] As for the intermediate between the deep-UV and visible region, UV NLO materials should have a minimum birefringence greater than 0.03, but a maximum that is smaller than 0.10. The birefringence ranges are considered suitable for optimal NLO performance in the UV region to achieve the PM condition and avoid the walk-off and self-focus effects. In the case of $Sr(NO_3)(NH_2SO_3)\cdot H_2O$, the incorporation of $[NO_3]$ and $[NH_2SO_3]$ groups effectively increases its birefringence compared to sulfamate-based materials, while maintaining a lower birefringence compared to nitrate-based materials (Figure 4b). Based on the measured birefringence, the PM wavelength of $Sr(NO_3)(NH_2SO_3)\cdot H_2O$ almost reaches the cutoff edge of 290 nm, creating a favorable condition for PM requirements and laser output efficiency. By striking a balance in the birefringence, $Sr(NO_3)(NH_2SO_3)\cdot H_2O$ proves to be desirable for UV NLO applications. First-principles calculations based on density-functional theory reveal that $Sr(NO_3)(NH_2SO_3)\cdot H_2O$ possesses an indirect bandgap of 3.66 eV (Figure S11, Supporting Information). The results of the total and partial density of states (DOS) indicate that the O-2*p* and N-2*p* orbitals primarily occupy the top of the valence bands and the bottom of the conduction bands, respectively. This suggests that the bandgaps of $Sr(NO_3)(NH_2SO_3)\cdot H_2O$ are determined by the interaction of N−O bonds in the $[NO_3]$ units (**Figure 5**a). The analysis of the electron localization function reveals a spherical distribution of electrons around the Sr atom, while the $[NO_3]$ units and $[NH_2SO_3]$ groups exhibit clear asymmetric lobes (Figure 5b

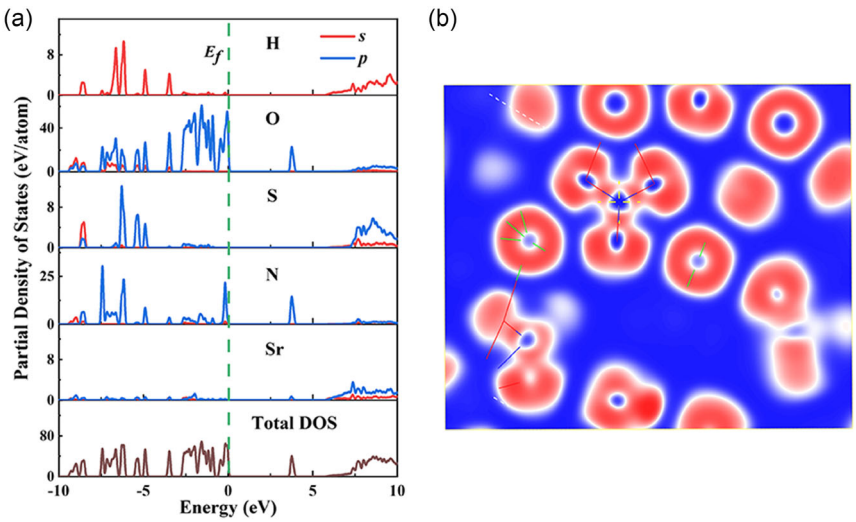

Figure 5. a) Partial density of states (DOS) and b) electron localization function analysis for $Sr(NO_3)(NH_2SO_3)\cdot H_2O$.

and S12, Supporting Information). This indicates that the $[NO_3]$ and $[NH_2SO_3]$ groups synergistically contribute to the anisotropy of the compound, thereby influencing its birefringence and SHG response.

In conclusion, the synthesis of the first nitrate sulfamate, $Sr(NO_3)(NH_2SO_3)\cdot H_2O$, with the NCS space group, $Pna2_1$, has been successfully achieved. $Sr(NO_3)(NH_2SO_3)\cdot H_2O$ exhibits SHG favorable zigzag $[SrNO_{10}(H_2O)]_\infty$ infinite layers and forms a honeycomb-like topology within its layered structure. This unique arrangement enhances the SHG response, resulting in a remarkable SHG response that is 5.1 times higher than that of KDP. Additionally, it demonstrates an improved birefringence ranging from 0.05709 to 0.07077 in the wavelength range of 406.7–1546.7 nm. The presence of interlayered covalent $[NH_2SO_3]$ groups plays a crucial role in promoting the growth of high-quality single crystals. As a result, $Sr(NO_3)(NH_2SO_3)\cdot H_2O$ crystals with dimensions of $19.0 \times 17.0 \times 3.5$ mm^3 have been obtained. This significant achievement introduces a new class of NLO materials and expands the frontiers of structural chemistry.

Supporting Information

Supporting Information is available from the Wiley Online Library or from the author.

Acknowledgements

X.W. and Y.L. contributed equally to this work. This research was supported by the National Research Foundation of Korea (NRF) funded by the Korea government (grant nos. 2018R1A5A1025208 and 2019R1A2C3005530), the National Natural Science Foundation of China (grant nos. 61835014 and 51972336), the National Key Research Project of China (grant no. 2022YFE0134500), National Science Foundation of United States (Awards DMR-19047012), and the Xinjiang Major Science and Technology Project (grant no. 2021A01001). The authors would like to express our sincere gratitude to Prof. Hongwei Yu for the generous assistance in the calculations of PM angles.

Conflict of Interest

The authors declare no conflict of interest.

Data Availability Statement

The data that support the findings of this study are available from the corresponding author upon reasonable request.

Keywords

birefringence measurements, nitrate sulfamates, nonlinear optical materials, second harmonic generation, ultraviolet

Received: July 20, 2023
Revised: August 27, 2023
Published online: September 13, 2023

[1] a) P. Becker, *Adv. Mater.* **1998**, *10*, 979; b) P. S. Halasyamani, K. R. Poeppelmeier, *Chem. Mater.* **1998**, *10*, 2753; c) K. M. Ok, E. O. Chi, P. S. Halasyamani, *Chem. Soc. Rev.* **2006**, *35*, 710; d) Y. Shen, S. Zhao, J. Luo, *Coord. Chem. Rev.* **2018**, *366*, 1; e) K. Wu, S. Pan, *Coord. Chem. Rev.* **2018**, *377*, 191; f) B. Zhang, G. Shi, Z. Yang, F. Zhang, S. Pan, *Angew. Chem., Int. Ed.* **2017**, *56*, 3916; g) M. Mutailipu, M. Zhang, H. Wu, Z. Yang, Y. Shen, J. Sun, S. Pan, *Nat. Commun.* **2018**, *9*, 3089.

[2] a) C. Chen, Y. Wu, A. Jiang, B. Wu, G. You, R. Li, S. Lin, *J. Opt. Soc. Am. B* **1989**, *6*, 616; b) C. Chen, Z. Xu, D. Deng, J. Zhang, G. K. L. Wong, B. Wu, N. Ye, D. Tang, *Appl. Phys. Lett.* **1996**, *68*, 2930; c) C. Chen, B. Wu, A. Jiang, G. You, *Sci. Sin. B* **1985**, *28*, 235; d) Y. Mori, I. Kuroda, S. Nakajima, T. Sasaki, S. Nakai, *Appl. Phys. Lett.* **1995**, *67*, 1818; e) Y. Wu, T. Sasaki, S. Nakai, A. Yokotani, H. Tang, C. Chen, *Appl. Phys. Lett.* **1993**, *62*, 2614; f) J. Chen, C.-L. Hu, F.-F. Mao, J.-H. Feng, J.-G. Mao, *Angew. Chem., Int. Ed.* **2019**, *58*, 2098; g) K. M. Ok, *Acc. Chem. Res.* **2016**, *49*, 2774; h) K. M. Ok, P. S. Halasyamani, D. Casanova, M. Llunell, P. Alemany, S. Alvarez, *Chem. Mater.* **2006**, *18*, 3176.

[3] a) M. Mutailipu, M. Zhang, B. Zhang, L. Wang, Z. Yang, X. Zhou, S. Pan, *Angew. Chem., Int. Ed.* **2018**, *57*, 6095; b) Z. Zhang, Y. Wang, B. Zhang, Z. Yang, S. Pan, *Angew. Chem., Int. Ed.* **2018**, *57*, 6577; c) X. Dong, L. Huang, C. Hu, H. Zeng, Z. Lin, X. Wang, K. M. Ok, G. Zou, *Angew. Chem., Int. Ed.* **2019**, *58*, 6528; d) S. Zhao, P. Gong, S. Luo, L. Bai, Z. Lin, Y. Tang, Y. Zhou, M. Hong, J. Luo, *Angew. Chem., Int. Ed.* **2015**, *54*, 4217.

[4] a) L. Chang, L. Wang, X. Su, S. Pan, R. Hailili, H. Yu, Z. Yang, *Inorg. Chem.* **2014**, *53*, 3320; b) H. Cheng, F. Li, Z. Yang, S. Pan, *Angew. Chem., Int. Ed.* **2022**, *61*, e202115669; c) S. G. Jantz, M. Dialer, L. Bayarjargal, B. Winkler, L. van Wüllen, F. Pielnhofer, J. Brgoch, R. Weihrich, H. A. Höppe, *Adv. Opt. Mater.* **2018**, *6*, 1800497; d) S. Schöenegger, S. G. Jantz, A. Saxer, L. Bayarjargal, B. Winkler, F. Pielnhofer, H. A. Höppe, H. Huppertz, *Chem. Eur. J.* **2018**, *24*, 16036; e) T. T. Tran, J. He, J. M. Rondinelli, P. S. Halasyamani, *J. Am. Chem. Soc.* **2015**, *137*, 10504.

[5] a) L. Xiong, J. Chen, J. Lu, C.-Y. Pan, L.-M. Wu, *Chem. Mater.* **2018**, *30*, 7823; b) P. Yu, L.-M. Wu, L.-J. Zhou, L. Chen, *J. Am. Chem. Soc.* **2014**, *136*, 480; c) S. Zhao, P. Gong, S. Luo, L. Bai, Z. Lin, C. Ji, T. Chen, M. Hong, J. Luo, *J. Am. Chem. Soc.* **2014**, *136*, 8560; d) Y. Li, F. Liang, S. Zhao, L. Li, Z. Wu, Q. Ding, S. Liu, Z. Lin, M. Hong, J. Luo, *J. Am. Chem. Soc.* **2019**, *141*, 3833.

[6] a) Z. Li, F. Zhang, W. Jin, Z. Yang, S. Pan, *Angew. Chem., Int. Ed.* **2022**, *61*, e202112844; b) Y. Sun, C. Lin, H. Tian, Y. Zhou, J. Chen, S. Yang, N. Ye, M. Luo, *Chem. Mater.* **2022**, *34*, 3781; c) Y. Zhou, X. Zhang, Z. Xiong, X. Long, Y. Li, Y. Chen, X. Chen, S. Zhao, Z. Lin, J. Luo, *J. Phys. Chem. Lett.* **2021**, *12*, 8280.

[7] a) Y.-Y. Li, W.-J. Wang, H. Wang, H. Lin, L.-M. Wu, *Cryst. Growth Des.* **2019**, *19*, 4172; b) Y. Pan, S.-P. Guo, B.-W. Liu, H.-G. Xue, G.-C. Guo, *Coord. Chem. Rev.* **2018**, *374*, 464; c) B. Zhang, E. Tikhonov, C. Xie, Z. Yang, S. Pan, *Angew. Chem., Int. Ed.* **2019**, *58*, 11726; d) X. Dong, Q. Jing, Y. Shi, Z. Yang, S. Pan, K. R. Poeppelmeier, J. Young, J. M. Rondinelli, *J. Am. Chem. Soc.* **2015**, *137*, 9417; e) M. Mutailipu, M. Zhang, Z. Yang, S. Pan, *Acc. Chem. Res.* **2019**, *52*, 791.

[8] a) M. Abudoureheman, L. Wang, X. Zhang, H. Yu, Z. Yang, C. Lei, J. Han, S. Pan, *Inorg. Chem.* **2015**, *54*, 4138; b) J.-L. Song, C.-L. Hu, X. Xu, F. Kong, J.-G. Mao, *Angew. Chem., Int. Ed.* **2015**, *54*, 3679; c) Y.-X. Ma, C.-L. Hu, B.-X. Li, F. Kong, J.-G. Mao, *Inorg. Chem.* **2018**, *57*, 11839; d) C. Wu, X. Jiang, Z. Wang, L. Lin, Z. Lin, Z. Huang, X. Long, M. G. Humphrey, C. Zhang, *Angew. Chem., Int. Ed.* **2021**, *60*, 3464.

[9] a) W. Huang, S. Zhao, J. Luo, *Chem. Mater.* **2022**, *34*, 5; b) W. Zhang, J. Huang, S. Han, Z. Yang, S. Pan, *J. Am. Chem. Soc.* **2022**, *144*, 9083; c) Z. Zhou, Y. Qiu, F. Liang, L. Palatinus, M. Poupon, T. Yang, R. Cong, Z. Lin, J. Sun, *Chem. Mater.* **2018**, *30*, 2203; d) Z. Li, W. Jin, F. Zhang, Z. Yang, S. Pan, *ACS Centr. Sci.* **2022**, *8*, 1557; M. Mutailipu, J. Han, Z. Li, F. Li, X. Long, Z. Yang, S. Pan, *Nat. Photonics* **2023**, *17*, 694.

[10] a) B. Cheng, Z. Li, Y. Chu, A. Tudi, M. Mutailipu, F. Zhang, Z. Yang, S. Pan, *Natl. Sci. Rev.* **2022**, *9*, nwac110; b) H. Wu, H. Yu, S. Pan, Z. Huang, Z. Yang, X. Su, K. R. Poeppelmeier, *Angew. Chem., Int. Ed.* **2013**, *52*, 3406; c) H. Yu, W. Zhang, J. Young, J. M. Rondinelli, P. S. Halasyamani, *Adv. Mater.* **2015**, *27*, 7380; d) G. Shi, Y. Wang, F. Zhang, B. Zhang, Z. Yang, X. Hou, S. Pan, K. R. Poeppelmeier, *J. Am. Chem. Soc.* **2017**, *139*, 10645; e) X. Wang, Y. Wang, B. Zhang, F. Zhang, Z. Yang, S. Pan, *Angew. Chem., Int. Ed.* **2017**, *56*, 14119; f) Y. Wang, B. Zhang, Z. Yang, S. Pan, *Angew. Chem., Int. Ed.* **2018**, *57*, 2150.

[11] a) X. Hao, M. Luo, C. Lin, G. Peng, F. Xu, N. Ye, *Angew. Chem., Int. Ed.* **2021**, *60*, 7621; b) X. Wang, J. Lee, Y. Li, Y. Kuk, K. M. Ok, *Inorg. Chem. Front.* **2023**, *10*, 1411.

[12] H. Tian, C. Lin, X. Zhao, S. Fang, H. Li, C. Wang, N. Ye, M. Luo, *Mater. Today Phys.* **2022**, *28*, 100849.

[13] a) X. Dong, L. Huang, Q. Liu, H. Zeng, Z. Lin, D. Xu, G. Zou, *Chem. Commun.* **2018**, *54*, 5792; b) P. Gross, Y. Zhang, L. Bayarjargal, B. Winkler, H. A. Höppe, *Dalton Trans.* **2022**, *51*, 11737; c) L. Huang, G. Zou, H. Cai, S. Wang, C. Lin, N. Ye, *J. Mater. Chem. C* **2015**, *3*, 5268; d) D. Dou, B. Cai, B. Zhang, Y. Wang, *Inorg. Chem.* **2022**, *61*, 21131.

[14] a) L. Li, Y. Wang, B.-H. Lei, S. Han, Z. Yang, K. R. Poeppelmeier, S. Pan, *J. Am. Chem. Soc.* **2016**, *138*, 9101; b) Y. Shen, Y. Yang, S. Zhao, B. Zhao, Z. Lin, C. Ji, L. Li, P. Fu, M. Hong, J. Luo, *Chem. Mater.* **2016**, *28*, 7110; c) S. Zhao, Y. Yang, Y. Shen, X. Wang, Q. Ding, X. Li, Y. Li, L. Li, Z. Lin, J. Luo, *J. Mater. Chem. C* **2018**, *6*, 3910; d) J. Chen, C. Lin, X. Jiang, G. Yang, M. Luo, X. Zhao, B. Li, G. Peng, N. Ye, Z. Hu, J. Wang, Y. Wu, *Mater. Horiz.* **2023**, *10*, 2876.

[15] P. Kubelka, F. Munk, *Z. Tech. Phys.* **1931**, *12*, 593.

[16] G. Peng, Y. Yang, Y.-H. Tang, M. Luo, T. Yan, Y. Zhou, C. Lin, Z. Lin, N. Ye, *Chem. Commun.* **2017**, *53*, 9398.

[17] S. K. Kurtz, T. T. Perry, *J. Appl. Phys.* **1968**, *39*, 3798.

[18] a) J. Stade, P. Held, L. Bohatý, *Cryst. Res. Technol.* **2001**, *36*, 347; b) A. Meinhart, E. Haussühl, L. Bohatý, E. Tillmanns, *Z. Kristallogr. Cryst. Mater.* **2009**, *216*, 513; c) G. Zou, C. Lin, H. G. Kim, H. Jo, K. M. Ok, *Crystals* **2016**, *6*, 42; d) L. Huang, G. Zou, H. Cai, S. Wang, C. Lin, N. Ye, *J. Mater. Chem. C* **2015**, *3*, 5268; e) X. Dong, L. Huang, Q. Liu, H. Zeng, Z. Lin, D. Xu, G. Zou, *Chem. Commun.* **2018**, *54*, 5792; f) G. Wang, M. Luo, N. Ye, C. Lin, W. Cheng, *Inorg. Chem.* **2014**, *53*, 5222; g) C. A. Ebbers, L. D. DeLoach, M. Webb, D. Eimerl, S. P. Velsko, D. A. Keszler, *IEEE J. Quantum Electron.* **1993**, *29*, 497; h) Y. Song, M. Luo, C. Lin, N. Ye, *Chem. Mater.* **2017**, *29*, 896; i) E. J. Cho, S. J. Oh, H. Jo, J. Lee, T. S. You, K. M. Ok, *Inorg. Chem.* **2019**, *58*, 2183; j) R. Cong, T. Yang, F. Liao, Y. Wang, Z. Lin, J. Lin, *Mater. Res. Bull.* **2012**, *47*, 2573.

[19] T. T. Tran, H. Yu, J. M. Rondinelli, K. R. Poeppelmeier, P. S. Halasyamani, *Chem. Mater.* **2016**, *28*, 5238.